

# Geometry of Acetylene and Ethylene Adsorbed on Cu(111): Theoretical Cluster Studies

By K. Hermann<sup>1\*</sup>, M. Witko<sup>2</sup> and A. Michalak<sup>3</sup>

<sup>1</sup> Fritz-Haber-Institut der MPG, Faradayweg 4–6, D-14195 Berlin, Germany

<sup>2</sup> Institute of Catalysis and Surface Chemistry, Polish Academy of Sciences, ul. Niezapominajek, 30239 Cracow, Poland

<sup>3</sup> Department of Computational Methods in Chemistry, Faculty of Chemistry, Jagiellonian University, R. Ingardena 3, 30060 Cracow, Poland

*Dedicated to Gerhard Ertl on the occasion of his 60th birthday*

(Received May 6, 1996)

## *Adsorption / Chemical bonding / Clusters / Quantum mechanics*

Recent experiments on acetylene and ethylene adsorbed at metal surfaces have shown that the adsorbates undergo major changes in their geometric structures while the overall adsorbate-substrate binding is weak. These findings can be explained by competitive adsorbate-substrate binding as evidenced in *ab initio* DFT and Hartree-Fock cluster studies using  $\text{Cu}_7(4,3)\text{Ad}$ ,  $\text{Ad} = \text{C}_2\text{H}_2, \text{C}_2\text{H}_4$ , clusters to simulate adsorption on Cu(111). The calculations confirm the increased C–C distances of both adsorbates found in the experiment and predict bending of the adsorbate CH and  $\text{CH}_2$  ends respectively near the surface which has not been observed so far. The distortion of the adsorbates is connected with rehybridization resulting in C–C bond weakening and increased adsorbate-substrate coupling. The latter can be characterized for both adsorbates by a Dewar-Chatt-Duncanson type donation scheme which is well known from organometallic chemistry.

Neuere Experimente zur Acetylen- und Ethylenadsorption an Metalloberflächen zeigen eine deutliche Geometrieänderung der Adsorbate, während die Adsorptionsenergie klein ausfällt. Dieses Ergebnis kann durch konkurrierende Beiträge zur Adsorbat-Substrat-Wechselwirkung erklärt werden, wie *ab initio* DFT- und Hartree-Fock-Clusteruntersuchungen zeigen. Die Rechnungen an den Clustern  $\text{Cu}_7(4,3)\text{Ad}$ ,  $\text{Ad} = \text{C}_2\text{H}_2, \text{C}_2\text{H}_4$ , welche die Adsorption an der Cu(111)-Oberfläche modellieren, bestätigen die in den Experimenten gefundene Vergrößerung des C–C-Abstands in beiden Adsorbaten und sagen eine Verkippung der CH- bzw.  $\text{CH}_2$ -Enden voraus. Die Verzerrung der Moleküle durch die Adsorption hat eine Rehybridisierung und damit eine vergrößerte Adsorbat-Substrat-Bindung zur Folge. Letztere wird in beiden Adsorbaten durch ein Dewar-Chatt-Duncanson-artiges Donationsschema beschrieben, das aus der organometallischen Chemie wohlbekannt ist.

## 1. Introduction

The adsorption of small organic molecules at metal surfaces is of considerable interest from both experimental and theoretical points of view as it

accounts for elementary steps in many important surface reactions connected with heterogeneous catalysis [1, 2]. A microscopic description of adsorption processes must always be based on realistic surface interaction mechanisms which derive conceptually from those of local adsorbate-substrate binding and from those of changes in the intramolecular binding of the adsorbate. Thus, energies connected with different surface binding schemes, ionic, covalent, Van der Waals type, have to be combined with those from changes in the intramolecular adsorbate binding to yield energies characterizing the global surface interaction of the molecular adsorbate. In many cases, molecular adsorption is accompanied by only minor effects on the intra-molecular electronic structure and the adsorbing molecule remains mostly unchanged in its geometry. Here an overall weak surface interaction reflects weak local adsorbate-substrate binding. This contrasts to systems where the adsorption process leads to a major geometric rearrangement in the adsorbing molecule. In these systems intra-molecular energy contributions cannot be neglected and the global surface interaction of the molecular adsorbate may not characterize the local adsorbate-substrate bond strength. Extreme cases of this type include dissociative adsorption where the adsorbate loses its identity near the surface [3, 4]. Other examples are systems where the geometric rearrangement in the adsorbing molecule requires energy which partially compensates the energy gain due to local bond formation between the distorted adsorbate molecule and the substrate surface (competitive binding). As a result, the global surface interaction of the molecular adsorbate may be quite weak while it cannot be described by Van der Waals type physisorption. Acetylene,  $C_2H_2$ , and ethylene,  $C_2H_4$ , adsorption on metal surfaces are candidates of this class of surface binding as will be discussed in the present paper.

Experimental results for acetylene and ethylene adsorption as well as ethylene dehydrogenation at 3d metal surfaces [5–11] identify a rather weak adsorbate-substrate interaction making it necessary to cool these systems to rather low temperatures in order to stabilize the adsorbates at the substrate surface. However, recent photoelectron diffraction (PED) and surface extended X-ray-adsorption fine-structure (SEXAFS) measurements have found major structural rearrangements in adsorbed  $C_2H_2$  on Cu(111) [5] and  $C_2H_4$  on Ni(111) [6, 7, 12] compared to the free molecules. The  $C_2H_2$  molecule which is linear in gas phase stabilizes over a bridge site on Cu(111) where the C–C axis points almost parallel to the surface and the two C centers point towards adjacent 3-fold fcc and hcp hollow sites [5]. The  $C_2H_4$  molecule which is planar in gas phase stabilizes with its C centers bridging nearest neighbor atom pairs (di- $\sigma$  orientation [13]) on Ni(111) [6, 7]. In both molecules the measured C–C distance,  $d_{C-C}$ , is increased by adsorption yielding  $d_{C-C} = 1.48 \pm 0.10$  Å for adsorbed vs.  $d_{C-C} = 1.20$  Å for free  $C_2H_2$  and  $d_{C-C} = 1.60 \pm 0.18$  Å for adsorbed vs.  $d_{C-C} = 1.34$  Å for free  $C_2H_4$ . Positions of the hydrogens in the adsorbates could not be ob-

served by the experiments due to their small scattering cross sections. They may, however, be of importance in the surface bond formation process as will be discussed below.

So far, theoretical studies on the  $C_2H_2$ /metal and  $C_2H_4$ /metal adsorption have been restricted to the cluster model approach where both semiempirical [14] and *ab initio* [15–19] techniques were applied. In early *ab initio* studies based on very small  $Me_nC_2H_2$ ,  $Me = Fe, Ni, Cu, n = 1–3$ , model clusters different adsorbate sites have been considered and the adsorbate geometry was varied within a limited range [15, 16]. The authors conclude for distorted  $C_2H_2$  (enlarged C–C distance, CH ends bent by  $30^\circ$  away from the surface) adsorbing at  $Cu_2$  and  $Cu_3$  clusters respectively that the local adsorbate-substrate bond can be described by a Dewar-Chatt-Duncanson type donation mechanism [20, 21]. This mechanism is well known from organometallic chemistry [13] and is found to weaken the C–C bond of the adsorbate in agreement with *ab initio* Hartree-Fock and configuration interaction calculations on a  $Cu_7(4,3)C_2H_2$  cluster representing the  $C_2H_2$ /Cu(111) adsorbate system [17]. It has also been confirmed in recent studies using correlated wavefunctions (*ab initio* Hartree-Fock + Møller-Plesset (MP2) corrected) on molecular  $Cu_nC_2H_2$ ,  $n = 1–4$ , compounds [22] as well as on  $Cu_nC_2H_2$ ,  $n = 4, 7, 22$ , and  $Pd_nC_2H_2$ ,  $n = 4, 7$ , surface clusters [18] simulating the  $C_2H_2$ /Cu(111) and  $C_2H_2$ /Pd(111) adsorbate systems. Further, cluster studies on  $Ni_{14}(C_2H_4)_2$  simulating the  $C_2H_4$ /Ni(110) adsorption and based on the density functional theory (DFT-LDA) approach [19] support the idea of a dative adsorbate-substrate binding connected with C–C bond weakening in the adsorbate and resulting in an increased C–C distance.

The present paper continues our previous cluster calculations on the  $C_2H_2$ /Cu(111) adsorbate system [17] and extends the study to  $C_2H_4$ /Cu(111) adsorption which forms an interesting addition in connection with the ethylene dehydrogenation process ( $C_2H_4 \rightarrow C_2H_2 + H_2$ ) at metal surfaces. Here the previous *ab initio* Hartree-Fock and configuration interaction calculations on a  $Cu_7(4,3)C_2H_2$  surface cluster [17] are complemented by DFT-LSDA studies on the same cluster and on  $Cu_7(4,3)C_2H_4$  representing the  $C_2H_4$ /Cu(111) adsorbate system. The emphasis of this work will be on binding geometries and a detailed quantitative discussion of the adsorption energetics carried out previously for  $Cu_7(4,3)C_2H_2$  [17, 18] will not be given. Geometry optimizations are performed for the adsorbates in the presence of the  $Cu_7(4,3)$  substrate cluster (with its structure fixed at the ideal Cu(111) surface geometry) using the experimentally [5, 6] identified  $C_s$  symmetry as a constraint.

For  $C_2H_2$ /Cu(111) the present calculations based on the DFT-LSDA approach confirm the experimental adsorbate orientation measured by PED [5] and yield good agreement with experiment for the adsorbate-substrate distance. Further, the calculated increase of the C–C distance in adsorbed vs. free  $C_2H_2$  reproduces the experiment. The calculations predict that both

CH ends of adsorbed  $C_2H_2$  are bent by about  $60^\circ$  to point away from the surface resulting in a strongly distorted adsorbate molecule which has not been observed so far. For  $C_2H_4/Cu(111)$  the DFT-LSDA calculations yield an adsorbate orientation which is identical to that of the  $C_2H_2/Cu(111)$  system whereas a di- $\sigma$  orientation observed by PED for the  $C_2H_4/Ni(111)$  system [6] is excluded in the calculations for Cu(111). However, the calculated increase of the C–C distance in adsorbed vs. free  $C_2H_4$  is consistent with experimental findings on  $C_2H_4/Ni(111)$  [6] and on  $C_2H_4/Cu(100)$  [12] as well as with theoretical results from cluster studies on  $C_2H_4/Ni(110)$ . Analogous to  $C_2H_2$  the calculations suggest that both  $CH_2$  ends of adsorbed  $C_2H_4$  are bent by about  $50^\circ$  which has not yet been confirmed experimentally.

The calculations suggest a very similar competitive adsorbate-substrate interaction scheme for  $C_2H_2/Cu(111)$  and  $C_2H_4/Cu(111)$  where the energy required to distort the adsorbate molecule is estimated from DFT calculations on the free molecules to yield 2.8 eV for  $C_2H_2$  and 1.9 eV for  $C_2H_4$ . The distortion of the adsorbates is connected with rehybridization resulting in C–C bond weakening and increased adsorbate-substrate binding. The latter can be characterized for both adsorbates by a Dewar-Chatt-Duncanson type donation/back-donation scheme [20, 21] involving the  $6a'$  HOMO's and  $7a'$  LUMO's of the adsorbates as well as Cu  $3d$ ,  $4sp$  orbitals.

In section 2 we describe details of the cluster geometries and of the methods used to calculate the electronic structure of the clusters. Section 3 presents the numerical results and discussion while section 4 summarizes conclusions from the present study.

## 2. Theoretical details

In the present study we use a  $Cu_7(4,3)$  substrate cluster of  $C_s$  symmetry, see Fig. 1, which forms a compact section of the ideal Cu(111) surface with four atoms of the first and three atoms of the second layer. The Cu–Cu nearest neighbor distance is taken from the bulk,  $d_{Cu-Cu} = 4.824$  Bohr. The  $Cu_7(4,3)$  substrate cluster is found to give a reliable description of electronic properties of different adsorbate systems at the Cu(111) surface [23, 24] and is, therefore, appropriate for the present purpose. Test calculations for acetylene adsorption on larger substrate clusters up to  $Cu_{22}(12,7,3)$  [17] and  $Cu_{30}(14,8,8)$  [18] have shown that adsorbate geometries and bonding are only minutely affected if larger clusters are used. To the  $Cu_7(4,3)$  cluster the adsorbate molecules,  $C_2H_2$  or  $C_2H_4$ , are added and their geometries are optimized keeping the substrate part of the cluster frozen.

In  $Cu_7(4,3)C_2H_2$  the  $C_2H_2$  adsorbate is placed on the  $C_s$  mirror plane of the substrate cluster, see Fig. 1 a. Here the adsorbate geometry starts from the linear free molecule ( $d_{C-C} = 2.247$  Bohr,  $d_{C-H} = 1.984$  Bohr) bending

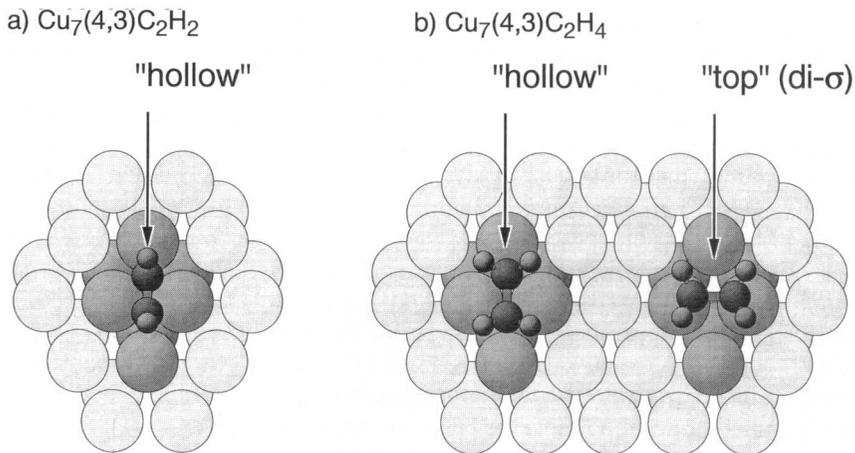


**Fig. 1.** Geometric structure of the  $\text{Cu}_7(4,3)\text{C}_2\text{H}_2$  and  $\text{Cu}_7(4,3)\text{C}_2\text{H}_4$  clusters used in the present study. The  $\text{C}_2\text{H}_2$  adsorbate in hollow geometry, Fig. 1a, bends over a Cu(111) bridge site with its two C centers pointing towards adjacent fcc and hcp hollow sites. For the  $\text{C}_2\text{H}_4$  adsorbate, Fig. 1b, two symmetries are considered, the hollow geometry (left cluster) and the top (di- $\sigma$ ) geometry (right cluster). The very light balls represent peripheral Cu substrate atoms which are meant to illustrate the Cu(111) surface geometry.

symmetrically over a Cu(111) bridge site with the C–C axis parallel to the surface and its two C centers pointing towards adjacent fcc and hcp hollow sites (geometry labeled “hollow” in Fig. 1a) in accordance with experimental results [5]. This geometry is further optimized allowing all adsorbate centers to rearrange along the mirror plane yielding a non-linear molecule as discussed below. In  $\text{Cu}_7(4,3)\text{C}_2\text{H}_4$  two  $\text{C}_2\text{H}_4$  adsorbate orientations are considered. In the first orientation, the adsorbate is placed with its C–C axis at the  $C_s$  mirror plane of the substrate cluster, see left part of Fig. 1b, where the adsorbate geometry starts from the planar free molecule ( $d_{\text{C-C}} = 2.505$  Bohr,  $d_{\text{C-H}} = 2.022$  Bohr) bending symmetrically over a Cu(111) bridge site (geometry labeled “hollow” in Fig. 1b) and is optimized allowing all adsorbate centers to rearrange such that the  $C_s$  mirror plane is conserved. This is analogous to the optimization performed for the  $\text{Cu}_7(4,3)\text{C}_2\text{H}_2$  cluster. In this orientation the  $\text{C}_2\text{H}_4$  molecule is found non-planar at the surface as discussed below. In the second orientation, the adsorbate is placed with its C–C axis parallel to a Cu–Cu nearest neighbor pair at the substrate surface, see right part of Fig. 1b, where the adsorbate geometry starts again from the planar free molecule with its C centers above the respective Cu centers (so-called di- $\sigma$  geometry [13] labeled “top” in Fig. 1b) and is optimized allowing all adsorbate centers to rearrange such that  $C_s$  mirror plane symmetry is conserved.

Two different methods have been used to determine the electronic structure of the clusters. In a first set of calculations the electronic structure and derived properties of the clusters are obtained with the *ab initio* density functional theory (DFT) method [25] using the local spin density approximation (LSDA) for exchange and correlation based on the Vosko-Wilk-Nusair functional [26]. The basis sets of contracted Gaussian orbitals (CGTO's) were all-electron type and taken from free atom DFT optimizations [27]. The results based on the DFT approach are complemented by a second set of data where cluster wave functions are calculated with the *ab initio* Hartree-Fock (HF) LCAO method [28] using flexible CGTO basis sets. The basis sets are all-electron type for the adsorbate atoms C [29] and H [30], while contracted valence basis sets [31] are used for the Cu substrate atoms with their  $Ar/3d^{10}$  cores approximated by effective core potentials (ECP's) [31]. The importance of basis set superposition errors (BSSE's) is estimated using the full counterpoise method [32] and turns out to be of minor importance for the present geometric considerations. Further, correlation contributions to the electronic structure are examined in separate studies on  $Cu_7(4,3)C_2H_2$  [17] and are found to affect binding energetics dramatically but influence adsorbate geometries only little. The comparison of DFT with HF results for the present clusters can give information about method specific differences.

The symmetry group common to  $Cu_7(4,3)C_2H_2$  and  $Cu_7(4,3)C_2H_4$  is described by  $C_s$ , see Fig. 1, and all electronic states are calculated based on  $C_s$  symmetry even if their proper symmetry is higher. As an illustration we mention the isolated adsorbate molecules where  $C_2H_2$  is characterized, apart from  $C_s$ , by  $D_{\infty h}$  (linear geometry) and by  $C_{2v}$  (bent geometry). Thus, the ground state configuration is described alternatively as  $^1A'(6a'^2 1a''^2)$  in  $C_s$ , as  $^1\Sigma_g(3\sigma_g^2 2\sigma_u^2 1\pi_u^2)$  in  $D_{\infty h}$ , or as  $^1A_1(4a_1^2 2b_1^2 1b_2^2)$  in  $C_{2v}$  symmetry where  $6a'$ ,  $1\pi_u$ ,  $4a_1$  refers to the highest occupied orbital (HOMO) and  $7a'$ ,  $1\pi_g$ ,  $2b_2$  refers to the lowest unoccupied orbital (LUMO). Analogously, the  $C_2H_4$  molecule is characterized, apart from  $C_s$ , by  $D_{2h}$  (planar geometry) and by  $C_{2v}$  (bent geometry). The ground state configuration is described alternatively as  $^1A'(6a'^2 2a''^2)$  in  $C_s$ , as  $^1A_g(3a_g^2 2a_u^2 1b_{3u}^2 1b_{2g}^2 1b_{2u}^2)$  in  $D_{2h}$ , and as  $^1A_1(4a_1^2 2b_1^2 1b_2^2 1a_2^2)$  in  $C_{2v}$  symmetry where  $6a'$ ,  $1b_{2u}$ ,  $4a_1$  denotes the HOMO and  $7a'$ ,  $1b_{3g}$ ,  $2b_2$  denotes the LUMO.

### 3. Results and discussion

Table 1 summarizes the computed geometry results of the free  $C_2H_2$  and  $C_2H_4$  molecules and of the respective adsorbate clusters  $Cu_7(4,3)C_2H_2$ ,  $Cu_7(4,3)C_2H_4$ . Here data from the density functional theory calculations (labeled "DFT" in the table) are compared with those of the Hartree-Fock approach (labeled "HF") as well as with available experimental data for the extended surface systems.

**Table 1.** Computed geometries of the free  $C_2H_2$  and  $C_2H_4$  molecules and of the respective adsorbate clusters  $Cu_7(4,3)C_2H_2$ ,  $Cu_7(4,3)C_2H_4$ . The density functional theory data (DFT) are compared with Hartree-Fock data (HF) and with experimental geometries derived from photoelectron diffraction on the surface systems  $C_2H_2/Cu(111)$  [5] and  $C_2H_4/Ni(111)$  [6]. The table contains results of the perpendicular C–Cu distances of each adsorbate C center with respect to the Cu surface,  $z_{C-Cu}$ , and of the C–C and C–H distances of the free molecules/adsorbates,  $d_{C-C}$  and  $d_{C-H}$ . Angle  $\theta(CCH)$  characterizes bending of the CH ends in  $C_2H_2$  while  $\theta(CCH_2)$  determines bending of the  $CH_2$  plane with respect to the surface plane. The two entries for  $z_{C-Cu}$ ,  $\theta(CCH)$ , and  $\theta(CCH_2)$  refer to the C centers closest to the fcc and hcp hollow surface sites, respectively. For further details see text. The  $Cu_7(4,3)C_2H_4$  results of this table refer to the “hollow” orientation of the adsorbate, see Fig. 1, while  $C_2H_4$  does not stabilize on  $Cu_7(4,3)$  in the “top” orientation. Note that experimental results on  $C_2H_4/Cu(111)$  do not exist and the  $C_2H_4/Ni(111)$  data refer to a different adsorbate/surface orientation compared to the cluster model.

	Free molecule		Adsorbate ( $Cu_7(4,3)Ad$ )		Experiment
	DFT	HF	DFT	HF	
(a) Ad = $C_2H_2$					
$z_{C-Cu}$ (Bohr)	–	–	2.632/2.765	2.693/2.688	$2.61/2.72 \pm 0.06$ [5]
$d_{C-C}$ (Bohr)	2.299	2.247	2.639	2.596	$2.80 \pm 0.19$ [5]
$d_{C-H}$ (Bohr)	2.047	1.984	2.097	2.045	–
$\theta(CCH)$ (Deg)	180.0	180.0	116.3/119.8	116.8/118.6	–
(b) Ad = $C_2H_4$					
$z_{C-Cu}$ (Bohr)	–	–	3.125/3.125	2.756/2.753	$(3.59 \pm 0.04)$ [6]
$d_{C-C}$ (Bohr)	2.522	2.505	2.877	2.973	$(3.02 \pm 0.34)$ [6]
$d_{C-H}$ (Bohr)	2.078	2.072	2.094	2.039	–
$\theta(CCH_2)$ (deg)	180.0	180.0	132.8/133.9	125.6/128.7	–

For free acetylene the linear equilibrium geometry ( $\theta(CCH) = 180^\circ$ ) is confirmed by the present DFT and HF calculations with interatomic C–C and C–H distances,  $d_{C-C}$  and  $d_{C-H}$ , in very good agreement with standard quantum chemical results [33]. When  $C_2H_2$  approaches the  $Cu_7(4,3)$  cluster along the  $C_s$  mirror plane the adsorbate stabilizes above the Cu surface with its molecular geometry greatly influenced. The DFT results yields a local equilibrium where the C–C axis points almost parallel to the surface. The perpendicular C–Cu surface distance of the C center closest to the fcc hollow site amounts to  $z_{C-Cu} = 2.63$  Bohr while  $z_{C-Cu} = 2.77$  Bohr for the C center closest to the hcp hollow site resulting in a bending of the C–C axis by only  $3^\circ$  with respect to the surface. In this orientation the C–C distance of the adsorbate,  $d_{C-C} = 2.64$  Bohr, is greatly increased with respect to that of the free molecule,  $d_{C-C} = 2.30$  Bohr while the C–H distances are affected only little. Further, the CH ends of the adsorbate are bent (away from the surface) by  $64^\circ$  ( $\theta(CCH) = 116^\circ$  near the fcc site) and  $63^\circ$  ( $\theta(CCH) = 117^\circ$  near the hcp site) respectively yielding a strongly non-linear molecule geometry.

The geometric structure of the adsorbed  $C_2H_2$  molecule given by  $d_{C-C}$ ,  $d_{C-H}$ , and  $\theta(CCH)$  and obtained in the DFT calculations agrees rather well with the present HF result, see Table 1, and with those of previous HF cluster studies [17, 18]. However, the calculated distances between the adsorbate and the substrate surface, quantified by two  $z_{C-Cu}$  values, are found quite different in the different treatments. Previous HF studies report optimized  $z_{C-Cu}$  values near 3.2 Bohr [17, 18] and an early Hartree-Fock-Slater-LCAO study on  $Cu_nC_2H_2$ ,  $n = 1-3$ , clusters uses even  $z_{C-Cu} = 3.59$  Bohr [16] which is considerably larger than the present data,  $z_{C-Cu} \approx 2.65$  Bohr, from both DFT and HF calculations. The origin of this discrepancy is not fully understood but may be connected with differences in the  $d$  orbital shape near the Cu substrate atoms. In the previous HF calculations Cu basis sets of all-electron type [17] or using an 11-electron ECP representation [18] are applied which yield  $d$  orbitals of similar spatial extent in the free Cu atom. These  $d$  orbitals are overall more diffuse than those obtained with the present all-electron Cu basis from free atom DFT optimizations [27]. On the other hand, the present HF treatment uses a one-electron ECP representation [31] of the substrate Cu atoms where the  $d$  electron part is known to represent quite contracted  $d$  orbitals compared to those of typical all-electron basis sets [34]. Altogether, the discrepancy between the present  $z_{C-Cu}$  values and those reported previously may be explained by the different extent of the  $d$  orbitals in the HF and DFT approach which allows the adsorbate molecule to stabilize closer to the surface in the DFT compared to the previous HF treatment.

The computed equilibrium geometry of adsorbed  $C_2H_2$  is compared in Table 1 with experimental results from photoelectron diffraction (PED) on the  $C_2H_2/Cu(111)$  adsorbate system [5]. The perpendicular C-Cu surface distances  $z_{C-Cu}$  of the DFT treatment are in very good agreement with respective experimental values. Both the absolute magnitudes of  $z_{C-Cu}$  and their differences between the C centers near the fcc and hcp hollow sites on Cu(111) agree well confirming the  $3^\circ$  bending of the C-C axis of  $C_2H_2$  with respect to the surface. Further, the increased C-C equilibrium distance,  $d_{C-C} = 2.64$  Bohr, found for  $Cu_7(4,3)C_2H_2$  differs from the experimental PED result for  $C_2H_2/Cu(111)$ ,  $d_{C-C} = 2.80 \pm 0.19$  Bohr, by only 5% and lies within the experimental error bars. Unfortunately, neither the calculated C-H distance nor the bending angle  $\theta(CCH)$  of the adsorbate can be compared with PED data for  $C_2H_2/Cu(111)$  since hydrogen positions cannot be observed in PED due to their small scattering cross sections [5]. As will be discussed below the bending of the CH ends in the adsorbate seems to form a major ingredient of the adsorbate-substrate binding. Thus, an experimental determination of  $d_{C-H}$  and  $\theta(CCH)$  would be highly desirable.

For free ethylene the planar equilibrium geometry is reproduced by the present DFT and HF calculations with interatomic C-C and C-H distances



which are, as for  $C_2H_2$ , in good agreement with standard quantum chemical results [33]. For  $C_2H_4$  approaching the  $Cu_7(4,3)$  cluster in the “top” orientation (di- $\sigma$  geometry) where the adsorbate is placed with its C–C axis parallel to a Cu–Cu nearest neighbor pair at the substrate surface, see right part of Fig. 1b, the adsorbate-substrate interaction is found to be always repulsive with no stable equilibrium near the surface. This result is particularly important in view of the experimental results as discussed below. When  $C_2H_4$  approaches the  $Cu_7(4,3)$  cluster in the “hollow” orientation (where the adsorbate is placed with its C–C axis along the  $C_s$  mirror plane of the cluster, see left part of Fig. 1b), the adsorbate stabilizes above the Cu surface with its molecular geometry changed dramatically with respect to that of free  $C_2H_4$ . The DFT results, see Table 1, yield a local equilibrium where the C–C axis points parallel to the surface with a perpendicular C–Cu surface distance of  $z_{C-Cu} = 3.12$  Bohr. The C–C distance of the  $C_2H_4$  adsorbate,  $d_{C-C} = 2.88$  Bohr, is greatly increased with respect to that of the free molecule,  $d_{C-C} = 2.52$  Bohr while differences in the C–H distances are negligible. Further, the  $CH_2$  ends of the adsorbate are bent away from the surface which can be quantified by bending angles of the  $CH_2$  planes with respect to the surface plane yielding  $47^\circ$  ( $\theta(CCH_2) = 133^\circ$  near fcc site,  $= 134^\circ$  near hcp site) and resulting in a non-planar molecule geometry.

The adsorption geometry of the  $C_2H_4$  molecule given by  $d_{C-C}$ ,  $d_{C-H}$ , and  $\theta(CCH_2)$  and obtained in the DFT calculations differs from that of the present HF results by less than 5%, see Table 1, while the equilibrium distance  $z_{C-Cu}$  is found to be smaller by 13% (0.37 Bohr) in the HF compared to the DFT approach. The latter may indicate the limitations in the present HF treatment discussed above. While theoretical studies on the  $C_2H_4/Cu(111)$  adsorbate system do not seem to exist so far LCGTO-LDF cluster studies on the  $C_2H_4/Ni(110)$  adsorbate system using  $Ni_{14}(C_2H_4)_2$  clusters [19] yield an increased C–C distance,  $d_{C-C} = 2.66$  Bohr, for the adsorbate and its  $CH_2$  ends bending away from the surface in consistence with our findings. However, the changes between free  $C_2H_4$  and the adsorbate reported in Ref. [19] are less pronounced than those of the present study which is very likely due to the different adsorbate surface orientations yielding the “top” orientation on Ni(110) (di- $\sigma$  geometry with  $C_2H_4$  stabilizing further away from the surface) as opposed to the “hollow” orientation on Cu(111) found to be preferred in the present system.

Due to lack of experimental data for the  $C_2H_4/Cu(111)$  adsorbate system the computed equilibrium geometry of adsorbed  $C_2H_4$  is compared in Table 1 with experimental PED results on the  $C_2H_4/Ni(111)$  adsorbate system [6]. The perpendicular C–Cu surface distances  $z_{C-Cu}$  of the DFT treatment for Cu(111) are smaller by 14% (0.47 Bohr) compared to the experimental result for Ni(111). This is explained by the fact that the experimental adsorbate orientation on Ni(111) is identified as di- $\sigma$  type (“top”

orientation, see right part of Fig. 1b) as opposed to the present calculations on Cu(111) where the “top” orientation is excluded and the “hollow” orientation is found most stable. The difference in C<sub>2</sub>H<sub>4</sub> adsorption on Cu(111) and Ni(111) is not obvious but most likely due to different *d* electron participation in the surface binding as a result of the open shell 3*d*<sup>9</sup> structure of Ni compared to closed shell 3*d*<sup>10</sup> for Cu. However, the increased C–C equilibrium distance,  $d_{C-C} = 2.88$  Bohr, found for Cu<sub>7</sub>(4,3)C<sub>2</sub>H<sub>4</sub> differs from the experimental PED result for C<sub>2</sub>H<sub>4</sub>/Ni(111),  $d_{C-C} = 3.02 \pm 0.34$  Bohr, by less than 5% and lies within the experimental error bars. This may suggest that the C–C distance is affected only little by the detailed surface orientation of the C<sub>2</sub>H<sub>4</sub> adsorbate. As further evidence we mention surface extended X-ray-absorption fine-structure (SEXAFS) measurements on the C<sub>2</sub>H<sub>4</sub>/Cu(100) adsorbate system [12]. These measurements find an increased C–C distance  $d_{C-C} = 2.78 \pm 0.14$  Bohr which lies within the range of the PED data for C<sub>2</sub>H<sub>4</sub>/Ni(111) [6] and agrees with the present theoretical C<sub>2</sub>H<sub>4</sub>/Cu(111) result. Analogous to the C<sub>2</sub>H<sub>2</sub>/Cu(111) system neither the calculated C–H distance nor the bending angle  $\theta(\text{CCH}_2)$  of the C<sub>2</sub>H<sub>4</sub> adsorbate can be compared with experimental data since hydrogen positions cannot be observed in PED nor in SEXAFS [6, 12]. As stated before bending of the CH<sub>2</sub> ends in the adsorbate seems to be of importance for the adsorbate-substrate binding which makes an experimental determination of  $d_{C-H}$  and  $\theta(\text{CCH}_2)$  highly desirable.

The sizable changes in the adsorbate structure of C<sub>2</sub>H<sub>2</sub> and C<sub>2</sub>H<sub>4</sub> on Cu(111) are combined with overall rather weak adsorbate-substrate binding as has been found in the experiment [5, 6] and discussed in previous cluster studies [17, 18]. This suggests for the two molecules a competitive surface binding scheme where the adsorbate-substrate interaction energy can be subdivided conceptually into contributions from two competing effects, (a) the geometric distortion of the molecule by adsorption which requires energy (distortion energy), and (b) the binding of the distorted molecule near the substrate surface which gains energy. Both contributions must be of similar magnitude with (b) being slightly larger than (a) such that overall the adsorbate binds weakly to the surface.

The distortion energy can be estimated roughly from total energy calculations on the free molecules neglecting additional rehybridization near the surface. Table 2 lists total energies  $E_{\text{tot}}$  of C<sub>2</sub>H<sub>2</sub> and C<sub>2</sub>H<sub>4</sub> obtained from the present DFT calculations where  $E_{\text{tot}}(\text{free})$  gives the result of the respective free molecule in its optimized geometry while  $E_{\text{tot}}(\text{ads.})$  refers to geometries optimized for the adsorbates binding to the Cu<sub>7</sub>(4,3) cluster. Further,  $\Delta E_{\text{tot}}$  denotes the energy difference  $\Delta E_{\text{tot}} = E_{\text{tot}}(\text{ads.}) - E_{\text{tot}}(\text{free})$  which corresponds to the above discussed distortion energy and yields  $\Delta E_{\text{tot}} = 2.8$  eV for C<sub>2</sub>H<sub>2</sub> and = 1.9 eV for C<sub>2</sub>H<sub>4</sub>. While the present values are somewhat too large due to overbinding in the DFT-LSDA approximation [25] their range and relative order is reasonable.

**Table 2.** Total energies  $E_{\text{tot}}$  of the  $\text{C}_2\text{H}_2$  and  $\text{C}_2\text{H}_4$  molecules obtained from the present DFT calculations. Here  $E_{\text{tot}}(\text{free})$  gives the result of the respective free molecule in its optimized geometry while  $E_{\text{tot}}(\text{ads.})$  refers to the geometry optimized for the adsorbate in the cluster, see Table 1, and  $\Delta E_{\text{tot}}$  denotes the energy difference  $\Delta E_{\text{tot}} = E_{\text{tot}}(\text{ads.}) - E_{\text{tot}}(\text{free})$ . Note that for numerical identification purposes the total energies are given with six digits which does not reflect the actual accuracy of the physical treatment of the systems.

	$\text{C}_2\text{H}_2$	$\text{C}_2\text{H}_4$
$E_{\text{tot}}(\text{free})$ (Hartree)	-76.598730	-77.840682
$E_{\text{tot}}(\text{ads.})$ (Hartree)	-76.496669	-77.772409
$\Delta E_{\text{tot}}$ (eV)	2.78	1.86

In hydrocarbon chemistry the electronic structure of (linear) acetylene,  $\text{C}_2\text{H}_2$ , is described by a  $\text{C}\equiv\text{C}$  triple bond and  $\text{C}-\text{H}$  binding deriving from  $sp$  hybridization near the carbon centers while (planar) ethylene,  $\text{C}_2\text{H}_4$ , is described by a  $\text{C}=\text{C}$  double bond and  $\text{C}-\text{H}_2$  binding resulting from  $sp^2$  hybridization. Further, ethane,  $\text{C}_2\text{H}_6$ , is described by a  $\text{C}-\text{C}$  single bond and  $\text{C}-\text{H}_3$  binding due to  $sp^3$  hybridization. In this spirit, distorting the  $\text{C}_2\text{H}_2$  molecule by bending its CH ends to yield the adsorbate geometry can be viewed conceptually as creating an incomplete  $\text{C}_2\text{H}_4$  molecule (with one hydrogen missing on each side) in its genuine geometry. This corresponds to an effective transition from a  $\text{C}-\text{C}$  triple to a weaker double bond and from  $sp$  to  $sp^2$  hybridization near the C centers of distorted  $\text{C}_2\text{H}_2$ . The resulting  $sp^2$  hybrid orbitals are not fully saturated making the C centers reactive and available for binding with the metal surface. This binding mechanism can also be applied to  $\text{C}_2\text{H}_4$  adsorption. Here distorting the  $\text{C}_2\text{H}_4$  molecule by bending its  $\text{CH}_2$  ends to yield the adsorbate geometry may be interpreted as creating an incomplete  $\text{C}_2\text{H}_6$  molecule (with one hydrogen missing on each side) in its genuine geometry. This would lead to an effective transition from a  $\text{C}-\text{C}$  double to a weaker single bond and from  $sp^2$  to  $sp^3$  hybridization near the C centers of distorted  $\text{C}_2\text{H}_4$ . As before, the resulting  $sp^3$  hybrid orbitals are not fully saturated making the C centers of  $\text{C}_2\text{H}_4$  available for binding with the metal surface.

The  $\text{C}-\text{C}$  bond weakening in  $\text{C}_2\text{H}_2$  and  $\text{C}_2\text{H}_4$  which originates from rehybridization as a result of the molecular distortion leads to increased  $\text{C}-\text{C}$  bond distances. The increased  $d_{\text{C}-\text{C}}$  values determined by the present cluster study and from experiments [5, 6] for the adsorbate systems, see Table 1, are fully consistent with the above interpretation. As an illustration we mention typical  $d_{\text{C}-\text{C}}$  values [35] obtained for  $\text{C}-\text{C}$  triple ( $d_{\text{C}=\text{C}} = 2.28$  Bohr), double ( $d_{\text{C}=\text{C}} = 2.56$  Bohr), and single bonds ( $d_{\text{C}-\text{C}} = 2.92$  Bohr). This suggests that the  $\text{C}-\text{C}$  bond in adsorbed  $\text{C}_2\text{H}_2$  ( $d_{\text{C}-\text{C}} = 2.6-2.8$  Bohr)

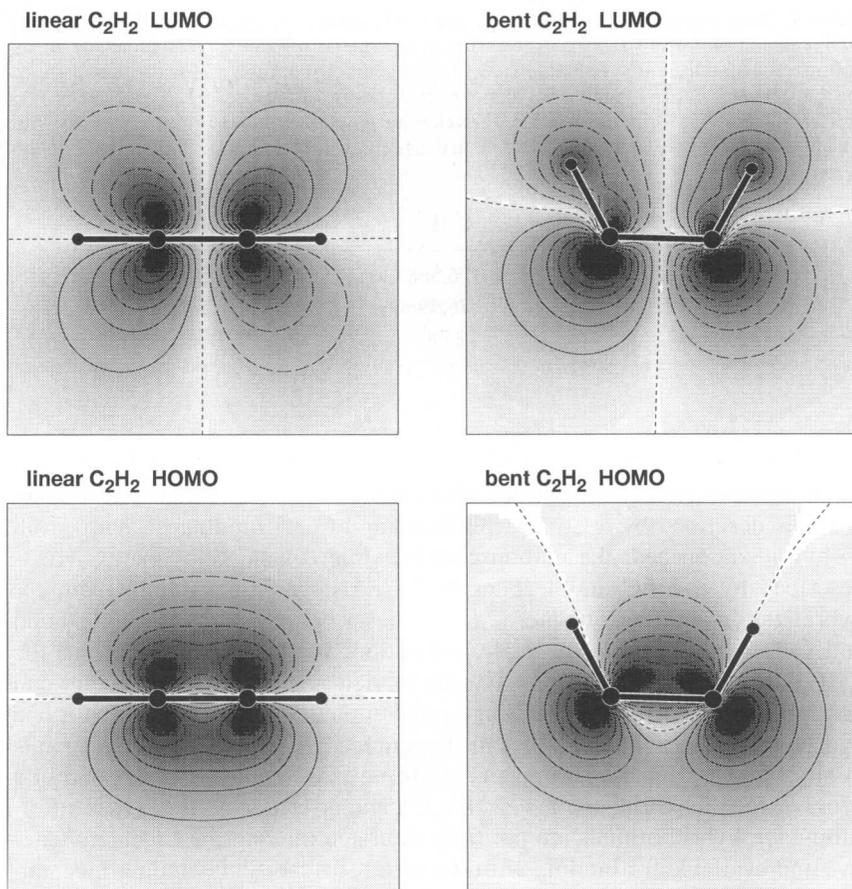


**Fig. 2.** Shaded contour plots of the highest occupied orbital (HOMO),  $6a'$  ( $1\pi_u$ ,  $4a_1$ ), and of the lowest unoccupied orbital (LUMO),  $7a'$  ( $1\pi_g$ ,  $2b_2$ ) of  $C_2H_2$  in its free molecule (linear) and adsorbate (bent) geometry. The contour plane contains all atom centers of the molecule marked by black dots. Full (dashed) lines refer to positive (negative) wave function values with contours ranging from  $-0.28$  au. to  $+0.28$  au. ( $1$  au. =  $1$  e/Bohr<sup>3</sup>) with equidistant increments of  $0.04$  au. The shaded overlay sketches the orbital density.

may be characterized as a double rather than triple bond and that of adsorbed  $C_2H_4$  ( $d_{C-C} = 2.9-3.0$  Bohr) may be better described as a single than a double bond.

Bond formation of the distorted  $C_2H_2$  and  $C_2H_4$  adsorbates with the Cu substrate surface happens in a similar way and can be described in detail by orbital and population analyses of the adsorbate clusters. Fig. 2 shows for free  $C_2H_2$  contour plots of the highest occupied orbital  $6a'$  (HOMO:

$1\pi_u$  in  $D_{\infty h}$ ,  $4a_1$  in  $C_{2v}$  symmetry) and of the lowest unoccupied orbital  $7a'$  (LUMO:  $1\pi_g$  in  $D_{\infty h}$ ,  $2b_2$  in  $C_{2v}$  symmetry) along a plane containing all atom centers of the molecule. In linear  $C_2H_2$  the HOMO (bottom left plot) is described by a bonding combination of C  $2p$  functions at the two C centers and contributes to the C–C triple bond in free acetylene. If the CH ends on both sides of the molecule are bent and the C–C distance increased to reflect the  $C_2H_2$  adsorbate geometry the HOMO (bottom right plot) admixes C  $2sp$  character such that its lobes at the C centers become asymmetric sticking out in a lone pair type fashion at the side adjacent to the Cu substrate. This effect can be connected with the  $sp$  to  $sp^2$  rehybridization described above and allows the HOMO of the adsorbing  $C_2H_2$  to easily mix with Cu  $3d$  and  $4sp$  orbitals resulting in a charge transfer (donation) from the adsorbate to the substrate. This charge transfer is partially compensated by a back-donation effect where Cu  $3d$  and  $4sp$  admix contributions of the adsorbate LUMO thereby transferring charge from the metal to the substrate. The LUMO which is described in the free  $C_2H_2$  as an anti-bonding combination of C  $2p$  functions (top left plot) is modified in the adsorbate geometry by additional C  $2sp$  contributions (top right plot) which increase its charge at the side adjacent to the Cu substrate and enhances its availability for back-donation.

The HOMO  $6a'$  ( $1b_{2u}$  in  $D_{2h}$ ,  $4a_1$  in  $C_{2v}$  symmetry) and LUMO  $7a'$  ( $1b_{3g}$  in  $D_{2h}$ ,  $2b_2$  in  $C_{2v}$  symmetry) of  $C_2H_4$  are in their orbital character very similar to the corresponding orbitals in  $C_2H_2$ . In fact, contour plots of the  $6a'$  and  $7a'$  orbitals in  $C_2H_4$  shown in Fig. 3 agree almost quantitatively with those of  $C_2H_2$  (Fig. 2). As a consequence, the qualitative rehybridization and combined donation/back-donation mechanism discussed above applies in the same way to  $C_2H_4$  and  $C_2H_2$  adsorption. The donation/back-donation scheme is well known from the theory of hydrocarbon-metal binding in complexes [13] and at surfaces [15–18, 36] and is recognized as the Dewar-Chatt-Duncanson scheme [20, 21]. It is completely analogous to the Blyholder scheme proposed for CO-metal binding in carbonyls and at surfaces [37, 38].

## 4. Conclusions

The present study on  $Cu_7(4,3)C_2H_2$  and  $Cu_7(4,3)C_2H_4$  clusters identifies interesting details of adsorbate-substrate bond formation in the respective adsorbate systems. For  $C_2H_2/Cu(111)$  the calculations confirm the experimental adsorbate orientation measured by PED [5] where the adsorbate stabilizes over a bridge site with its C–C axis almost parallel to the surface and the two C centers pointing towards adjacent 3-fold fcc and hcp hollow sites. Further, the calculated increase of the C–C distance in adsorbed vs. free  $C_2H_2$  agrees with experiment. The calculations predict that both CH

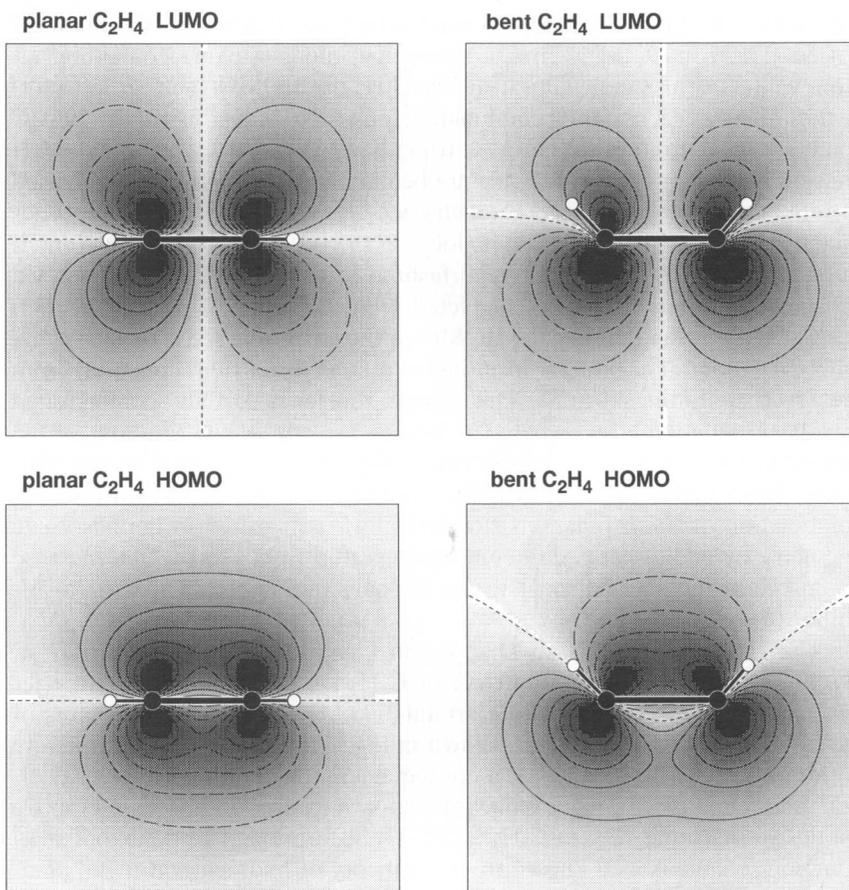


**Fig. 3.** Shaded contour plots of the highest occupied orbital (HOMO),  $6a'$  ( $1b_{2u}, 4a_1$ ), and of the lowest unoccupied orbital (LUMO),  $7a'$  ( $1b_{3g}, 2b_2$ ) of  $C_2H_4$  in its free molecule (planar) and adsorbate (bent) geometry. The contour plane forms a mirror plane of the molecule containing its two C centers (marked by black dots) and lies perpendicular to the atom plane of free  $C_2H_4$ . The H centers (marked by circles) are placed symmetrically above and below the contour plane. Full (dashed) lines refer to positive (negative) wave function values with contours ranging from  $-0.28$  au. to  $+0.28$  au. ( $1$  au. =  $1 e/\text{Bohr}^3$ ) with equidistant increments of  $0.04$  au. The shaded overlay sketches the orbital density.

ends of adsorbed  $C_2H_2$  are bent (by about  $60^\circ$ ) and point away from the surface which has not been observed so far but is in agreement with theoretical values published recently [17, 18].

For  $C_2H_4/\text{Cu}(111)$  which has not yet been examined experimentally the calculations yield an adsorbate orientation which is identical to that of the

$C_2H_2/Cu(111)$  system whereas a di- $\sigma$  orientation observed by PED for the  $C_2H_4/Ni(111)$  system [6] is excluded by the calculations for Cu(111). The latter discrepancy may be due to different  $d$  electron participation in the surface binding as a result of the open shell  $3d^9$  structure of Ni compared to closed shell  $3d^{10}$  for Cu. The calculated increase of the C–C distance in adsorbed vs. free  $C_2H_4$  is consistent with the experimental findings of PED studies on  $C_2H_4/Ni(111)$  [6] as well as with SEXAFS studies on  $C_2H_4/Cu(100)$  [12]. Analogous to  $C_2H_2$  the calculations suggest that both  $CH_2$  ends of adsorbed  $C_2H_4$  are bent (by about  $50^\circ$ ) pointing away from the surface which has not yet been found experimentally but is in qualitative agreement with cluster studies for  $C_2H_4/Ni(110)$  [19].

In both systems the adsorbate-substrate interaction is described by a competitive binding scheme consisting conceptually of two contributions, the geometric distortion of the molecule by adsorption which requires energy, and the binding of the distorted molecule near the substrate surface which gains energy. Both contributions must be of similar magnitude such that overall the adsorbate binds weakly to the surface. The distortion energy is roughly estimated from DFT calculations on the free molecules yielding 2.8 eV for  $C_2H_2$  and 1.9 eV for  $C_2H_4$ . Further, binding of the distorted molecules with the surface is found in the calculations to be very similar in character. It is described by a Dewar-Chat-Duncanson [20, 21] donation/back-donation mechanism involving the  $6a'$  HOMO's and  $7a'$  LUMO's of the adsorbates as well as Cu  $3d$ ,  $4sp$  orbitals.

The present work needs to be further substantiated by systematic studies including more complex geometry variations of the adsorbate and substrate as well as a larger set of substrate clusters differing in size and shape [23, 24, 38] to become fully convincing for the real surface systems. Detailed calculations along these lines are in progress [17, 39]. Further, the present calculations cannot describe the dynamics of the adsorption process which involves concerted adsorbate geometry variations and possible reaction barriers along the adsorption path. However, this study confirms that hydrocarbon adsorbate systems are interesting examples of a surface interaction determined by competitive effects which combine major geometry changes of the adsorbate with an overall weak adsorbate-substrate binding. As another candidate we mention benzene adsorption on metal surfaces where recent DLEED investigations on  $C_6H_6/Pt(111)$  [40] indicate weak adsorbate bonding connected with noticeable changes in the C–C distances.

### Acknowledgement

The authors are grateful for valuable discussions with A. M. Bradshaw. This work was funded in parts by the Deutsche Forschungsgemeinschaft and by Fonds der Chemischen Industrie. Further support was based on grant No. 3T09A11708 from the State Committee for Scientific Research of Poland.

## References

1. See e.g. *Surface Science and Catalysis*, Vol. 45, Eds. B. Delmon and J. T. Yates, Elsevier, Amsterdam 1989.
2. G. A. Somorjai, *Introduction to Surface Chemistry and Catalysis*, John Wiley, New York 1994.
3. K. Hermann, K. Freihube, T. Greber, A. Böttcher, R. Grobecker, D. Fick and G. Ertl, *Surf. Sci.* **313** (1994) L806.
4. T. Greber, K. Freihube, R. Grobecker, A. Böttcher, K. Hermann and G. Ertl, *Phys. Rev.* **B50** (1994) 8755.
5. S. Bao, K.-M. Schindler, P. Hofmann, V. Fritzsche, A. M. Bradshaw and D. P. Woodruff, *Surf. Sci.* **291** (1994) 295.
6. S. Bao, P. Hofmann, K.-M. Schindler, V. Fritzsche, A. M. Bradshaw, D. P. Woodruff and M. C. Asensio, *J. Phys.: Condens. Matter* **6** (1994) L93.
7. S. Bao, P. Hofmann, K.-M. Schindler, V. Fritzsche, A. M. Bradshaw, D. P. Woodruff, C. Casado and M. C. Asensio, *Surf. Sci.* **323** (1995) 19.
8. J. E. Demuth and D. E. Eastman, *Phys. Rev. Lett.* **32** (1974) 1123.
9. S. Lehwald and H. Ibach, *Surf. Sci.* **89** (1979) 425.
10. L. Hammer, T. Hertlein and K. Müller, *Surf. Sci.* **178** (1986) 693.
11. N. Sheppard, *Ann. Rev. Phys. Chem.* **39** (1988) 589.
12. D. Arvanitis, L. Wenzel and K. Baberschke, *Phys. Rev. Letters* **59** (1987) 2435.
13. M. R. Albert and J. T. Yates, *The Surface Scientist's Guide to Organometallic Chemistry*, ACS Publishing, Washington 1987.
14. A. B. Anderson, *J. Am. Chem. Soc.* **99** (1977) 696.
15. P. Geurts and A. van der Avoird, *Surf. Sci.* **102** (1981) 185.
16. P. Geurts and A. van der Avoird, *Surf. Sci.* **103** (1981) 416.
17. K. Hermann and M. Witko, *Surf. Sci.* **337** (1995) 205.
18. A. Clotet and G. Pacchioni, *Surf. Sci.* **346** (1996) 91.
19. M. Weinelt, W. Huber, P. Zebisch, H.-P. Steinrück, M. Pabst and N. Rösch, *Surf. Sci.* **271** (1992) 539.
20. M. J. S. Dewar, *Bull. Soc. Chim. France* **18** (1951) C79.
21. J. Chatt and L. A. Duncanson, *J. Chem. Soc.* (1953) 2939.
22. M. Böhme, T. Wagner and G. Frenking, *J. Organomet. Chem.*, in press.
23. K. Hermann, M. Witko, L. G. M. Pettersson and P. Siegbahn, *J. Chem. Phys.* **99** (1993) 610.
24. M. Witko and K. Hermann, *J. Chem. Phys.* **101** (1994) 10173.
25. see *Density Functional Methods in Chemistry*, J. K. Labanowski and J. W. Anzelm (eds.), Springer-Verlag, New York 1991. For the present calculations the DeMon program system was used. DeMon was developed by A. St-Amant and D. Salahub (University of Montreal) and is available from these authors.
26. S. H. Vosko, L. Wilk and M. Nusair, *Can. J. Phys.* **58** (1980) 1200.
27. N. Godbout, D. R. Salahub, J. Andzelm and E. Wimmer, *Can. J. Phys.* **70** (1992) 560.
28. For the present calculations the HONDO program system (version 8.3) was used to obtain Hartree-Fock wave functions. HONDO is a set of general purpose quantum chemical programs developed by M. Dupuis, A. Marquez, and E. Hollauer (IBM Corporation, Kingston) and available from these authors.
29. F. B. Van Duijneveldt, IBM Research Report No. RJ 945, 1971 (unpublished).
30. C. W. Bauschlicher, P. S. Bagus and H. F. Schaefer III, *IBM J. Res. Develop.* **22** (1978) 213.
31. P. S. Bagus, C. W. Bauschlicher, C. J. Nelin, B. C. Laskowski and M. Seel, *J. Chem. Phys.* **81** (1984) 3594.
32. S. F. Boys and F. Bernardi, *Mol. Phys.* **19** (1970) 553.



33. See e.g. *A Bibliography of Ab Initio Molecular Wave Functions*, Eds. W. G. Richards, T. E. H. Walker and R. K. Hinkley, Clarendon Press, Oxford 1971.
34. A. J. H. Wachters, *J. Chem. Phys.* **52** (1970) 1033.
35. R. T. Morrison and R. N. Boyd, *Organic Chemistry*, 3<sup>rd</sup> Ed., Allyn and Bacon Inc., Boston 1990.
36. A. B. Anderson, *J. Am. Chem. Soc.* **99** (1977) 696.
37. G. Blyholder, *J. Phys. Chem.* **68** (1964) 2772.
38. K. Hermann, P. S. Bagus and C. J. Nelin, *Phys. Rev.* **B35** (1987) 9467.
39. M. Witko, A. Michalak and K. Hermann, in preparation.
40. A. Wander, G. Held, R. Q. Hwang, G. S. Blackman, M. L. Xu, P. de Andres, M. A. Van Hove and G. A. Somorjai, *Surf. Sci.* **249** (1991) 21.